



Published in final edited form as:

Microcirculation. 2018 November ; 25(8): e12502. doi:10.1111/micc.12502.

Induction of microvascular network growth in the mouse mesentery

Ariana D. Suarez-Martinez^{1,2}, Shayn M. Peirce³, Brant E. Isakson⁴, Matthew Nice¹, Jack Wang², Karen M. Lounsbury⁵, Joshua P. Scallan⁶, Walter L. Murfee^{1,2}

¹Department of Biomedical Engineering, Tulane University, New Orleans, Louisiana

²Department of Biomedical Engineering, University of Florida, Gainesville, Florida

³Department of Biomedical Engineering, University of Virginia, Charlottesville, Virginia

⁴Department of Molecular Physiology & Biological Physics, University of Virginia, Charlottesville, Virginia

⁵Department of Pharmacology, Larner College of Medicine, University of Vermont, Burlington, Vermont

⁶Department of Molecular Pharmacology & Physiology, University of South Florida, Tampa, Florida

Abstract

Objective—Motivated by observations of mesenteries harvested from mice treated with tamoxifen dissolved in oil for inducible gene mutation studies, the objective of this study was to demonstrate that microvascular growth can be induced in the avascular mouse mesentery tissue.

Methods—C57 BL /6 mice were administered an IP injection for five consecutive days of: saline, sunflower oil, tamoxifen dissolved in sunflower oil, corn oil, or peanut oil.

Results—Twenty-one days post-injection, zero tissues from saline group contained branching microvascular networks. In contrast, all tissues from the three oils and tamoxifen groups contained vascular networks with arterioles, venules, and capillaries. Smooth muscle cells and pericytes were present in their expected locations and wrapping morphologies. Significant increases in vascularized tissue area and vascular density were observed when compared to saline group, but sunflower oil and tamoxifen group were not significantly different. Vascularized tissues also contained LYVE-1-positive and Prox1-positive lymphatic networks, indicating that lymphangiogenesis was stimulated. When comparing the different oils, vascularized tissue area and vascular density of sunflower oil were significantly higher than corn and peanut oils.

Correspondence: Walter L. Murfee, J. Crayton Pruitt Family Department of Biomedical Engineering, University of Florida, Gainesville, FL. wmurfee@bme.ufl.edu.

CONFLICT OF INTEREST

None.

SUPPORTING INFORMATION

Additional supporting information may be found online in the Supporting Information section at the end of the article.

Conclusions—These results provide novel evidence supporting that induction of microvascular network growth into the normally avascular mouse mesentery is possible.

Keywords

angiogenesis; lymphangiogenesis; microcirculation; microvascular network; mouse mesentery

1 | INTRODUCTION

The rat mesentery has been invaluable for advancing our understanding of the microcirculation. The thinness of the mesentery has provided unique views of the network, vessel, and cellular levels that remain largely unobtainable with other tissues. From vasoreactivity, immunohistochemistry, and more recently, ex vivo tissue culture studies, the use of the rat mesentery has provided insights into cell-cell interactions, phenotypic dynamics, basic network architecture, and dysfunction associated with multiple disease scenarios.^{1–8} Observations made in the rat mesentery in many ways have helped define the fundamental areas of microvascular research focused on hemodynamics, white blood cell mechanics, red blood cell flow, and microvascular network remodeling.^{3,5,9–11} Utilizing this tissue has shed light on different endothelial cell and pericyte phenotypes^{4,7,12–16} and network responses to various growth factors.^{1,17–19} Further, the tissues' characteristics have allowed for the investigation and manipulation of vessel-specific hemodynamic stresses,^{3,20–22} and for the observation of leukocyte responses to altered environments.^{3,5,11} The tissue has also offered fundamental characterization of microvascular innervation and the structure of initial lymphatic networks.^{8,23}

Intriguingly, the analogous transparent, connective tissue in the mouse is avascular.²⁴ A critical question remains: Can we induce microvascular growth into the mouse mesentery? Preliminary observations of mouse mesentery tissues treated with tamoxifen dissolved in oil for conditional gene mutation studies suggest that this is a possibility. Therefore, the overall objective of this study was to stimulate angiogenesis into the avascular mouse mesentery. Based on undocumented observations of vessel-like structures post intraperitoneal injections of tamoxifen dissolved in oil for conditional genetic mouse studies, and sparse examples from the literature,^{25,26} we specifically tested the hypothesis that tamoxifen treatment causes microvascular growth into the avascular mouse mesentery connective tissue. The presence of microvessels was quantified post-injection of tamoxifen, saline, sunflower oil, corn oil, or peanut oil following a typical, widely used protocol for inducible gene mutation studies. Our results provide evidence for the presence of branching, multicellular microvascular networks in the mouse mesentery. Microvascular growth was induced with tamoxifen along with the three different oils indicating that oil alone is sufficient for inducing microvascular network growth. While the mechanisms of microvascular growth remain to be determined, our results provide a new technical innovation for vascularizing the mouse mesentery. The stimulation of microvascular growth into the otherwise avascular, adult mouse mesentery tissue will provide a useful model that can be coupled with transgenic mice to inspire a new line of foundational studies for advancing our understanding of the microcirculation.

2 | MATERIALS AND METHODS

2.1 | Inducing microvascular growth in mouse mesentery tissue

All animal experiments were approved by Tulane University's or University of Florida's Institutional Animal and Care Use Committee. The procedure followed is a common protocol for tamoxifen induction in genetically engineered mice. Briefly, adult, female C57BL/6 mice were given a single intraperitoneal (IP) injection daily for 5 consecutive days. All injections were 0.1 mL in volume and warmed to 37°C. The experimental groups receiving injections were as follows: saline (n = 4 mice), sunflower oil (n = 4 mice), and tamoxifen (n = 4 mice), sterile sunflower oil (n = 4 mice), sterile corn oil (n = 3 mice), and sterile peanut oil (n = 3 mice). Mesentery tissues for these groups were harvested 21 days after the last injection. In addition to the stimulus experimental groups, there were two time point experimental groups for the sterile sunflower oil stimulus: 10 Days (n = 2) and 42 Days (n = 2). Sterile saline (Baxter), autoclaved and non-autoclaved organic sunflower oil (Spectrum), autoclaved corn oil (Sigma-Aldrich), autoclaved organic peanut oil (Spectrum), and 10 mg/mL of tamoxifen T5649 (Sigma-Aldrich) were utilized. To prepare tamoxifen, 5 mg of tamoxifen and 0.5 mL of non-sterile organic sunflower oil were added in a 1-mL centrifuge tube. Tamoxifen was dissolved by placing the tube on a shaker inside an oven set to 37°C for 2 hours.

2.2 | Harvesting and culturing mouse mesentery tissue

The mice were euthanized in a CO₂ chamber by asphyxiation followed by cervical dislocation. Similar to a previously established protocol by Stapor et al, 2013, the mesentery tissues were harvested. Briefly, the abdominal fur was shaved before sterilizing the abdomen with 70% isopropyl alcohol followed by 3 wipes with iodine. The abdominal skin and muscles were cut off with sterile scissors to expose the abdominal cavity. Using sterile techniques, the ileum was located as a reference point, and the mesentery was carefully spread on a sterile drape to expose the individual windows. Sterile saline, warmed to 37°C, was dripped on the tissue to keep it from drying out. Utilizing microscissors and forceps, mesenteric windows were aseptically harvested. Once removed, most tissues were rinsed in phosphate-buffered saline (PBS) and immediately fixed in 100% methanol. The tissues to be cultured were rinsed in sterile Dulbecco's phosphate-buffered saline (DPBS) and transferred to sterile minimum essential media containing Earle's Salts (MEM; Gibco) and 1% Penicillin-Streptomycin (PenStrep; Gibco) warmed to 37°C. In a biosafety cabinet, the tissues were transferred to a 6-well culture plate with 4 mL of culture media in each well. Culture media contained sterile MEM, 1% PenStrep, and 20% fetal bovine serum (FBS). Tissues were then placed inside an incubator set to standard cell culture conditions (5% CO₂, 37°C) for 3 days, where the media was changed every 24 hours.

2.3 | Immunohistochemistry

Before labeling, tissues were spread on a microscope slide and fixed in 100% methanol at -20°C for 30 minutes. Briefly, all antibodies were diluted in an antibody buffer solution containing PBS, 0.1% saponin, and 2% bovine serum albumin. Tissues were incubated with all primary and secondary antibodies for 1 hour at room temperature; conjugated Lectin was incubated 30 minutes. Tissues were then rinsed for 10 minutes three times with PBS and

0.1% saponin cooled to 4°C. The following antibodies were used to label the tissues: 1:200 mouse platelet endothelial cell adhesion molecule (PECAM; BD Biosciences) with 1:500 streptavidin secondary (Strep-CY2 or Strep-CY3, Jackson Immuno Research), 1:200 CY3-conjugated α -smooth muscle actin (α SMA, Sigma-Aldrich), 1:100 rabbit neuron-glia antigen 2 (NG2, Millipore) with 1:100 goat anti-rabbit secondary (GAR-594, Jackson Immuno Research), 1:100 rabbit lymphatic vessel endothelial hyaluronan receptor-1 (LYVE-1, AngioBio) with 1:100 GAR-CY3, 1:100 rabbit polyclonal Prox1 (Prox1, AngioBio) with 1:100 GAR-594, 1:100 FITC-conjugated rat CD11b (CD11b, BD Pharmingen), and 1:40 FITC-conjugated BSI-lectin (Lectin, Sigma-Aldrich).

2.4 | Image acquisition

Images were taken with a 4x, 10x, and 20x (oil) objectives from an inverted microscope Olympus IX71 paired with a Photometrics CoolSNAP EZ camera, or from an inverted microscope, Nikon Eclipse Ti2, paired with a Photometrics CoolSNAP DYNO camera. The bright field image was acquired with a Nikon dissecting microscope paired with a color camera. Whole tissue images of PECAM labeling were acquired with a 10 \times objective to be able to quantify microvascular growth.

2.5 | Quantification of microvascular growth

From each group, eight mesentery tissues were randomly chosen and imaged to be analyzed. All quantifications were performed via blind analysis. Using the Java-based NIH ImageJ²⁷ v.1.0 image processing software, the percentage of vascularized tissue area and vascular density of the mesentery tissues were determined. The vascular area of each tissue was measured by outlining the perimeter of the vasculature within the window. The outline included open-ended vascular segments and excluded vessels in the adipose border. The tissue area was measured by outlining the entire window excluding the adipose border. The areas were calculated in mm² based on the pixel to mm ratio of the image. The vascular area was then divided by the tissue area and converted to a percentage to calculate the vascularized tissue area. For vascular density, the number of segments per vascular area of a distinct network in the tissue was calculated. A segment was defined as the length of blood vessel between two nodes, defined as the branching points in the vascular network, where the segments do not have blind ends. A distinct network constituted of an arteriolar and venular pair with its corresponding capillaries. To differentiate between arterioles and venules, the diameter and morphology of endothelial cells were examined as arterioles have smaller diameters and more elongated endothelial cells due to their higher shear stress compared to venules.^{15,28}

2.6 | Statistical analysis

Data are presented as mean \pm standard error of mean (SEM). Oneway analysis of variance (ANOVA) test followed by Tukey's multiple comparisons test was used to analyze differences between three groups. Welch's unequal variances *t* test was used to analyze differences between sterile and non-sterile sunflower oil stimulation. GraphPad Prism version 7 software was used for all statistical analyses. Statistical significance was achieved when *P*-value < 0.05.

3 | RESULTS

3.1 | Sunflower oil and tamoxifen induce vascularization in mouse mesentery

After injecting mice with saline, sunflower oil, or tamoxifen for 5 consecutive days and harvesting tissues 21 days post-injection, the mesenteries from the saline group were still avascular (Figure 1 A), while the mesenteries from the non-sterile sunflower oil and tamoxifen groups contained complete microvascular networks (Figure 1 B,C). Here, we define the “mesenteric windows” as the thin, translucent connective tissue located between artery/vein pairs that feed the small intestine. The PECAM-positive endothelial cells lined the microvascular networks which contained a distinct hierarchy with branched arterioles, venules, and capillaries (Figure 1 B,C). Vessel types could be identified based on their endothelial cell morphologies and vessel diameters.^{15,28} Moreover, the newly formed microvessels across the hierarchy of microvascular networks in the mesenteric windows appear to be perfused with red blood cells (Figure 1 D). Every mesenteric window from the non-sterile sunflower oil (8/8) and tamoxifen (8/8) groups contained microvascular networks with arterioles, venules, and capillaries. In contrast, zero mesenteric windows (0/8) from the saline group contained a branching microvascular network. The percentages of vascularized tissue area for the Sunflower Oil and Tamoxifen group were dramatically increased compared to avascular Saline group (Figure 1 E, Saline: $0.0462 \pm 0.0462\%$; Sunflower Oil: $28.3 \pm 8.61\%$, $P = 0.0338$; Tamoxifen: $35.6 \pm 9.46\%$, $P = 0.0073$). A similar trend was observed when vascular density was compared. The number of segments per vascular area was significantly higher for the Sunflower Oil and Tamoxifen compared to Saline (Figure 1 F, Saline: $4.19 \pm 4.19 \text{ \#/mm}^2$; Sunflower Oil: $290 \pm 32.0 \text{ \#/mm}^2$, $P < 0.0001$; Tamoxifen: $275 \pm 31.8 \text{ \#/mm}^2$, $P < 0.0001$). Importantly, even though the size of each microvascular network from the Sunflower Oil and Tamoxifen groups varied, all the microvasculature was connected to vessels that originated from the periphery of the tissue, suggesting ingrowth from the surrounding adipose border.

3.2 | Multiple cell types are present in vascularized mouse mesentery

The microvasculature that grew into the mesentery tissues also contained perivascular cells. Including α SMA-positive smooth muscle cells and NG2-positive pericytes (Figure 2 A–F), along with CD11b-positive macrophages residing in the interstitial space (Figure 2 M–O). The two perivascular cells displayed common wrapping morphologies and were present in their expected locations. Moreover, along with the vascularization of the mesentery, tissues also displayed the growth of LYVE-1-positive (Figure 2 G–I), Prox1-positive (Figure 2 J–L) lymphatics. Lymphatics were distinguished by LYVE-1-positive or Prox1-positive labeling, intensity of PECAM, and endothelial cell morphology.

3.3 | Vascularization is induced by 10 days and sustained after 21 days

After injecting mice with sunflower oil for 5 consecutive days, tissues were harvested after 10 days (Figure 3 A), 21 days (Figure 3 B), or 42 days (Figure 3 C) post the last injection. PECAM-positive microvascular networks were present by Day 10. The vascularized tissue area significantly increased on Day 21 and 42 when compared to Day 10 (Figure 3 D, Day 10: $17.7 \pm 4.13\%$; Day 21: $61.6 \pm 7.22\%$, $P < 0.0001$; Day 42: $57.6 \pm 3.61\%$, $P < 0.0001$), but did not increase between Day 21 and 42 ($P = 0.8529$). In contrast, an opposite trend was

observed when vascular density was compared. The number of segments per vascular area was significantly higher for Day 10 compared to Day 21 and Day 42 (Figure 3 E, Day 10: $428 \pm 88.2 \text{ \#/mm}^2$; Day 21: $186 \pm 23.1 \text{ \#/mm}^2$, $P = 0.0106$; Day 42: $127 \pm 9.26 \text{ \#/mm}^2$, $P = 0.0017$), but comparable between Day 21 and Day 42 ($P = 0.7167$).

3.4 | Sunflower oil induces a higher vascularization area than corn or peanut oil

Sterile sunflower oil, corn oil, or peanut oil injections for 5 consecutive days stimulated microvascular growth evident by the presence of PECAM-positive networks (Figure 4 A–C). Quantification revealed that sunflower oil stimulation caused a significantly higher vascularized tissue area compared to corn and peanut oil, but no significant difference between corn and peanut oil (Figure 4 E, Sunflower Oil: $61.6 \pm 7.22\%$; Corn Oil: $16.6 \pm 4.78\%$, $P < 0.0001$; Peanut Oil: $27.0 \pm 5.89\%$, $P = 0.0016$). Vascular density, quantified as the number of segments per vascular area, was comparable between all three oil groups (Figure 4 F, Sunflower Oil: $186 \pm 23.1 \text{ \#/mm}^2$; Corn Oil: $144 \pm 13.4 \text{ \#/mm}^2$; Peanut Oil: $135 \pm 19.2 \text{ \#/mm}^2$, $P > 0.05$).

3.5 | Angiogenesis is stimulated ex vivo after stimulation

Recently, the culturing of rat mesentery was introduced as a novel ex vivo model for investigating real-time cell dynamics involved in angiogenesis across the hierarchy of an intact network.^{8,28} This motivated us to culture mouse mesentery tissues to observe whether angiogenesis can also be stimulated ex vivo, which would enable further experimental approaches using knockout and transgenic mice. Our results demonstrated that when mouse mesentery tissues from the Sunflower Oil or Tamoxifen groups were cultured for 3 days in MEM supplemented with 20% FBS, angiogenesis, defined as capillary sprouts, was indeed observed (Figure 5). When compared to Day 0 uncultured tissues, (Figure 5 A, C), Day 3 cultured tissues (Figure 5 B, D) displayed more capillary sprouts which are blind-ended PECAM-positive endothelial cell segments protruding from existing microvessels.

4 | DISCUSSION

The primary finding of this study is the induction of microvascular network growth into the avascular mouse mesentery, thus enabling the use of genetically modified mice to address the signaling pathway regulating angiogenesis and lymphangiogenesis. The rat mesentery is a thin connective tissue that provides an essential 2-dimensional view of intact 3-dimensional microvascular networks down to the single cell level. Mesenteries can be used for intravital microscopy⁷ are easily harvested for immunohistochemical labeling and can even be cultured.⁸ Our findings enable the combination of two fundamental tools for microcirculation research: the mesentery tissue and knockout/transgenic mouse strains.

The new microvascular networks in the mouse mesentery contained α SMA-positive smooth muscle cells and NG2-positive pericytes wrapping the capillaries. In addition, our observations indicated the presence of LYVE-1-positive or Prox1-positive lymphatic endothelial cells comprising the lymphatic system. Therefore, angiogenesis and lymphangiogenesis were induced in the mesentery after 21 days from the last injection. Twenty-one days was selected for the endpoint of this study based on typical tamoxifen

injection protocols for inducible knockout studies, but microvascular growth was present by 10 days. Furthermore, growth continued out to Day 21 which was then sustained to at least 42 days. The remodeling in the mesentery is also supported by the presence of apparent, activated NG2-positive, and LYVE-1-positive interstitial cells. LYVE-1-positive interstitial cells were nucleated but not all nucleated interstitial cells were LYVE-1-positive (Figure S1 B–D). The LYVE-1-positive cells were also lectin-positive (Figure S1 A–D). CD11b and DAPI labeling suggests that a subset of interstitial cells are macrophages (Figure S1 E–H). Overall, the observations of these different interstitial cell populations further support the use of the mouse mesentery to probe multicellular dynamics during angiogenesis and lymphangiogenesis.

The endothelial extensions along capillary sprouts in the mouse mesentery tissues displayed similar morphologies to sprouts in rat mesentery tissues.²⁹ While some sprouts displayed filopodia (Figure S2 C–D), they were more commonly characterized by blunt-ended pseudopodia extensions (Figure S2 A–B) similar to the capillary sprouts in angiogenic microvascular networks from rat mesentery.²⁹ Interestingly, in the rat mesentery networks, VEGFR-2 and UNC5b labeling along capillary sprouts did not differ between leading tip cells and stack cells.²⁹ Compared to reports from the literature characterizing tip cell identity and morphology,^{30–33} our observations in mouse and rat mesentery tissues suggest that capillary sprouting in adult mesentery tissue might follow an alternative paradigm.

The novelty of our findings is highlighted by the discovery of a robust method to induce microvascular network growth (angiogenesis and lymphangiogenesis) in the mouse mesentery, which is considered to be avascular.²⁴ This discovery establishes a platform for follow-up studies aimed at both using the model and better understanding it. While we do not yet know whether the new microvascular networks are more pathological or physiological, trial experiments indicate that vessel growth in the avascular mouse mesentery might be stimulus specific. For example, injections of compound 48–80 (a mast cell degranulator) did not cause vessel growth after 10 days (Figure 6 A). There were no PECAM-positive microvasculature networks in any of the 17 mesenteric windows that were harvested. In contrast, IP injection of ovarian cancer cells did induce angiogenesis (Figure 6 B). Together, these results suggest that microvascular growth effect in mouse mesentery tissues is stimulus dependent, yet not oil specific. While the unknown mechanisms remain a limitation, the mouse mesentery model enables the investigation of cell dynamics during angiogenesis and lymphangiogenesis across the hierarchy of an intact adult microvascular network with arterioles, capillaries, and venules in a tissue that can be whole mounted for immunolabeling and used for intravital microscopy. We believe this advantage of the mouse mesentery model is unique and offers a valuable tool for future research.

Searching “mouse mesentery” and “angiogenesis” in the literature using PubMed, only 29 results appear. Of these, there are fewer examples that suggest microvascular vessels can exist within the thin connective tissue and further support that microvascular growth is not oil specific. Norrby et al³⁴ report that compound 48–80 IP injections in mice led to a significant increase in angiogenesis within the mesenteric windows compared to its control. Anghelina et al³⁵ describe the stimulation of capillary sprouts into the mesentery tissue via VEGF injection or mechanical irritation. Studies by Van Steenkiste et al and Calderone et

al^{36,37} use the partial portal vein ligation model to research angiogenesis in mouse mesentery. Similar to our trial results, Dvorak and colleagues identify the extension of blood vessels toward tumors within mouse mesenteric windows 5 days after injecting cancer cells.³⁸ Also, Jeon et al³⁹ showed that the IP injection of ovarian cancer cells induces lymphangiogenesis.

The current study was in part inspired by undocumented light microscopy observations of apparent vessel structures in mesenteries from tamoxifen-treated mice for conditional gene knockout studies. Together with examples from the literature suggesting that tamoxifen can upregulate pro-angiogenic factors,^{25,26} these preliminary observations motivated the hypothesis that injecting tamoxifen into the peritoneal cavity of mice would be the cause for stimulating angiogenesis in the mesentery. However, our results reject this hypothesis and support that oil alone is sufficient to induce angiogenic growth. Sunflower oil was used as a control since it is a common solvent for tamoxifen. All 16 tissues, 8 from non-sterile sunflower oil and tamoxifen groups, contained at least one microvascular network comprised of a distinct arteriole, venule, and associated capillaries that extended from the adipose border to the thin connective tissue. In contrast, none of the saline tissues contained a microvascular network. Since saline-stimulated tissues remained avascular, our results clearly demonstrate that the induction of microvascular growth is associated with an oil-mediated response.

The effect of sunflower oil also prompted additional experiments to discover if angiogenesis and lymphangiogenesis were oil type specific. After following the same injection protocols, the effects of sterile sunflower, corn, and peanut oils were compared. These findings reveal that corn and peanut oil also induce microvascular growth into the avascular mouse mesentery with branching microvascular networks, perivascular cells, and lymphatic vessels being present for the three different oil types. The angiogenic property of oils is supported by previous experiments showing an increase in angiogenesis in wound healing of the skin when oils were applied.^{40,41} Oil also seemed to stimulate adipogenesis in the mesentery since adipose cell clusters in the window area were observed in tissues from all three different oils but not in the saline tissues. We speculate that the oil stimulation of angiogenesis was not tissue specific as the mesometrium within the peritoneal cavity displayed examples of increased microvascular density and sprouting (data not shown) when compared to unstimulated mesometrium.⁴² Our findings show that corn and peanut oil also induced microvascular growth into the avascular mouse mesentery tissue (Figure 4); yet interestingly, there is a significant decrease in the vascularized tissue area of corn and peanut oils when compared to sunflower oil. The differences highlight the unknown mechanisms with the oil types and motivate future experiments aimed at understanding what is sufficient to cause microvascular growth.

As microvascular growth and remodeling are common denominators for multiple pathologies such as diabetic retinopathy, myocardial ischemia, and tumor growth,⁴³ a need still exists to fully comprehend the multicellular dynamics during angiogenesis, which is defined as the growth of new blood vessels from existing ones. Ideal experimental models enable the observation and tracking of specific cell types at different temporal stages of growth at certain locations across a microvascular network. Our results also support the

culturing of mouse mesentery tissues for the future real-time tracking cell dynamics. In the context of tool development, ex vivo biomimetic models have emerged as powerful experimental platforms for basic science discovery and pre-clinical drug testing. A challenge for microvascular research, however, is recapitulating the complexity associated with intact networks in real tissue scenarios. To meet this challenge, our laboratory has recently introduced the rat mesentery culture model, which has the following advantages: (a) investigation of multicellular interactions, including endothelial cells, smooth muscle cells, pericytes, and macrophages,^{8,44,45} (b) similar to in vivo, angiogenesis most commonly occurs along venules and capillaries versus arterioles,⁸ (c) perivascular cells such as smooth muscle cells and pericytes remain functional during culture,^{8,46,47} and (d) the ability to capture time-lapse images during angiogenesis and lymphangiogenesis at the same time.^{44,48} Relevant to the contribution of the current study, the most common question motivated by the presentation of the rat mesentery culture model is—Can mouse mesentery be used? Similar to the rat mesentery tissue, the mouse mesentery is a self-contained tissue that can easily be cultured without the need of a 3-dimensional matrix gel platform, yet it is avascular. Thus, in order to use mouse mesentery tissue for culture applications, it must first be vascularized and our results provide a protocol to do so.

5 | CONCLUSIONS AND PERSPECTIVE

In summary, these results introduce a technical innovation that motivates the use of mouse mesentery connective tissue for investigating the microvascular growth and remodeling. The vascularized mouse mesentery can be viewed as an alternative platform to the rat mesentery for studying angiogenesis. Since the rat mesentery has shown to be invaluable for a myriad of microcirculation experiments, we foresee that this mouse mesentery model can offer similar impactful discoveries for researchers by enabling real-time cell fate and mechanistic studies of intact microvascular networks from genetically manipulated strains.

Supplementary Material

Refer to Web version on PubMed Central for supplementary material.

ACKNOWLEDGMENTS

Dr. Murfee would like to thank Dr. Stryder Meadows, Angela Crist, and Katie Huang for sharing their laboratory's experience with the tamoxifen IP injection protocols.

Funding information

Research reported in this publication was supported by the National Institute of Aging under Award Number R01AG049821.

Abbreviations

ANOVA	analysis of variance
DAPI	4',6-Diamidino-2-Phenylindole
DPBS	Dulbecco's phosphate-buffered saline

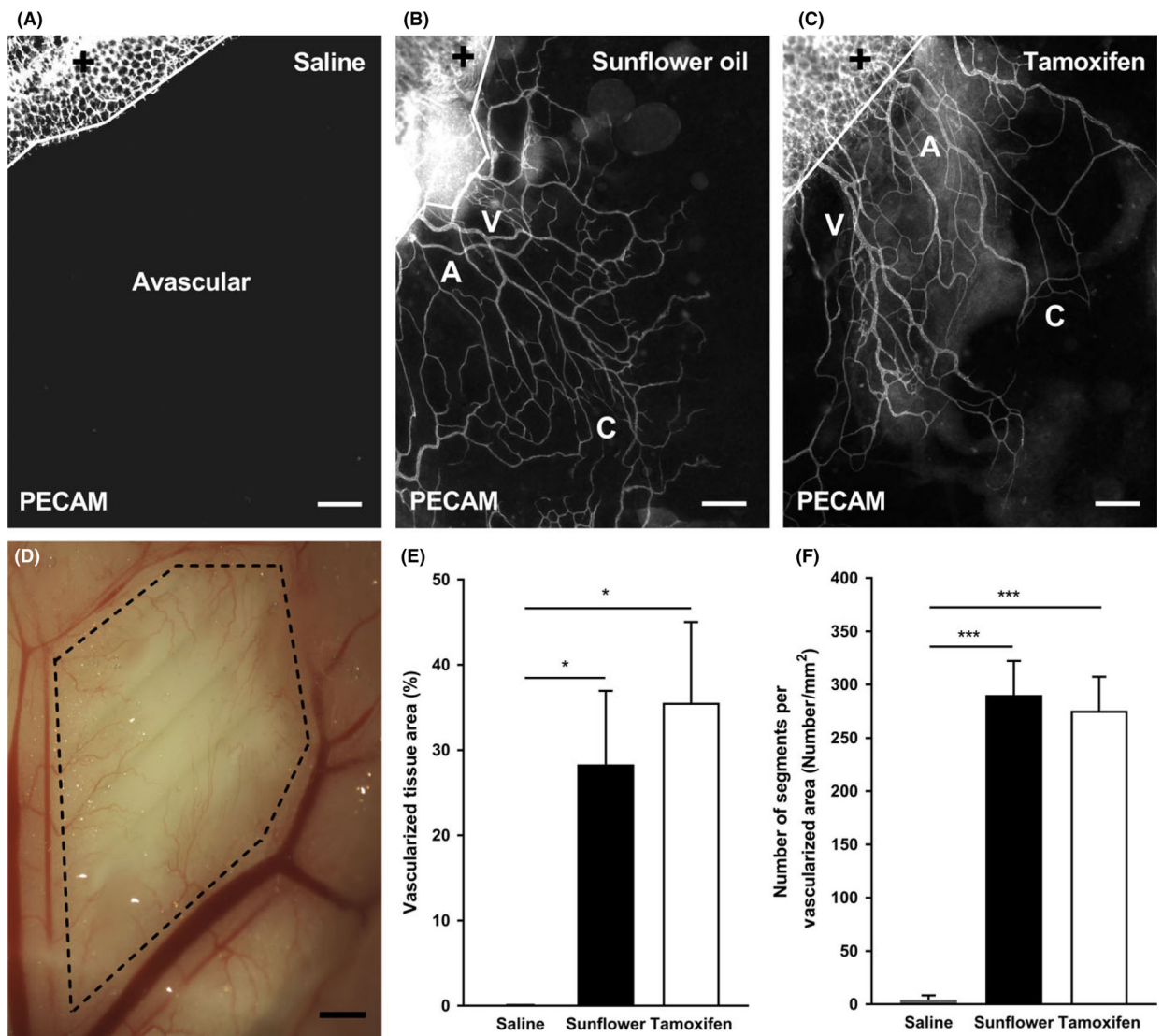
FBS	fetal bovine serum
GAR	goat anti-rabbit
IP	Intraperitoneal
LYVE-1	lymphatic vessel endothelial hyaluronan receptor-1
MEM	minimum essential media
NG2	neuron-glia antigen 2
PBS	phosphate-buffered solution
PECAM	platelet endothelial cell adhesion molecule
PenStrep	Penicillin-Streptomycin
SEM	standard error of mean
αSMA	smooth muscle actin- α

REFERENCES

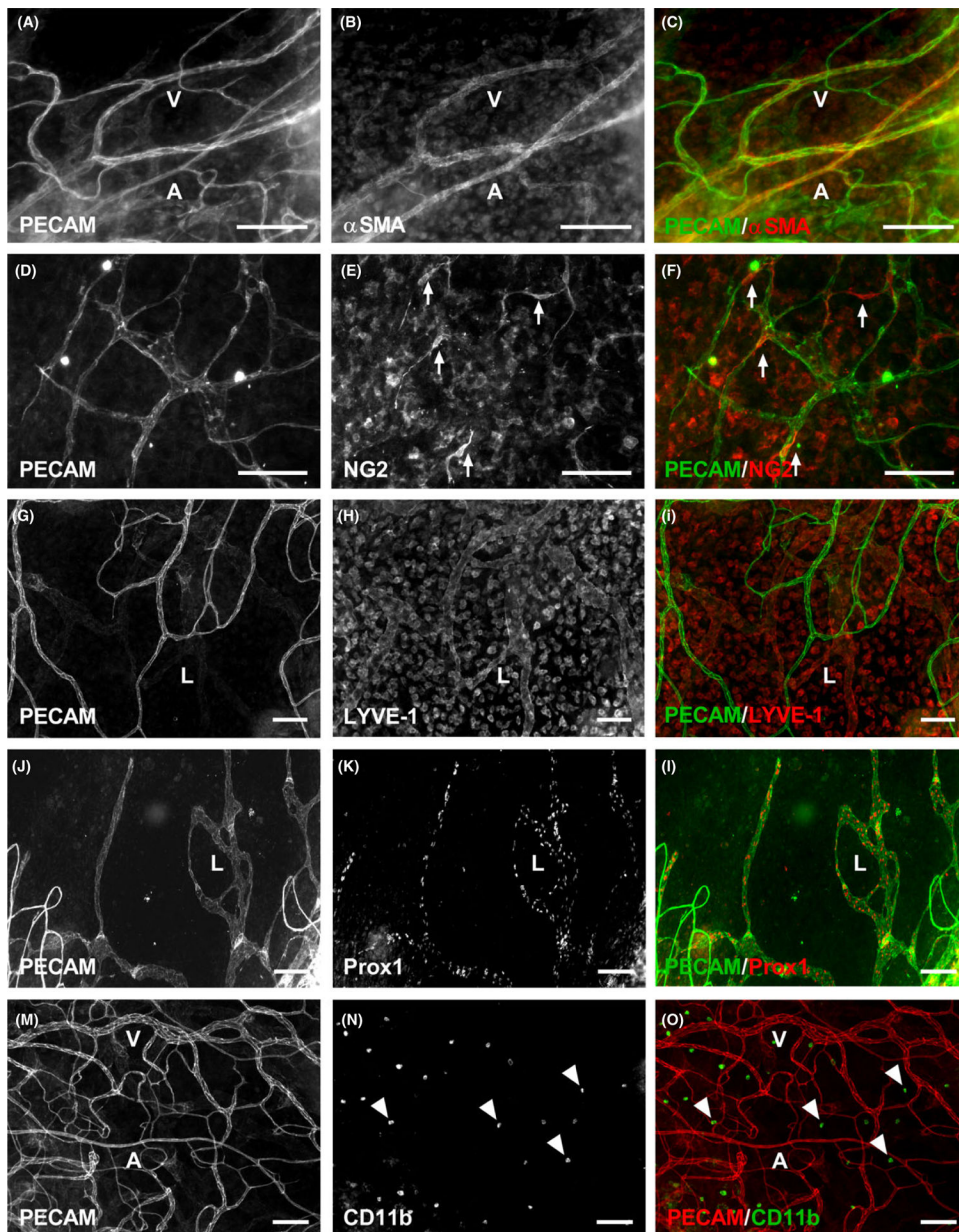
1. Breslin JW, Gaudreault N, Watson KD, Reynoso R, Yuan SY, Wu MH. Vascular endothelial growth factor-C stimulates the lymphatic pump by a VEGF receptor-3-dependent mechanism. *Am J Physiol Heart Circ Physiol.* 2007; 293:H709–H718. [PubMed: 17400713]
2. Costa JJ, Harris AG, Delano FA, Zweifach BW, Schmid-schönbein GW. Mast cell degranulation and parenchymal cell injury in the rat mesentery. *Microcirculation.* 1999; 6:237–244. [PubMed: 10501097]
3. Moazzam F, DeLano FA, Zweifach BW, Schmid-Schönbein GW. The leukocyte response to fluid stress. *Proc Natl Acad Sci.* 1997; 94 : 5338–5343. [PubMed: 9144238]
4. Nehls V, Drenckhahn D. Heterogeneity of microvascular pericytes for smooth muscle type alpha-actin. *J Cell Biol.* 1991; 113:147–154. [PubMed: 2007619]
5. Pearson MJ, Lipowsky HH. Influence of erythrocyte aggregation on leukocyte margination in postcapillary venules of rat mesentery. *Am J Physiol Heart Circ Physiol.* 2000; 279 : H1460–H1471. [PubMed: 11009430]
6. Ponce AM, Price RJ. Angiogenic stimulus determines the positioning of pericytes within capillary sprouts in vivo. *Microvasc Res.* 2003; 65: 45–48. [PubMed: 12535871]
7. Rhodin J, Fujita H. Capillary growth in the mesentery of normal young rats-Intravital video and electron microscope analyses. *J Submicrosc Cytol Pathol.* 1989; 21:1–34. [PubMed: 2702606]
8. Stapor PC, Azimi MS, Ahsan T, Murfee WL. An angiogenesis model for investigating multicellular interactions across intact microvascular networks. *Am J Physiol Heart Circ Physiol.* 2013; 304:1235–1245.
9. Pries AR, Secomb TW. Modeling structural adaptation of microcirculation. *Microcirculation.* 2008; 15:753–764. [PubMed: 18802843]
10. Secomb TW, Styp-Rekowska B, Pries AR. Two-dimensional simulation of red blood cell deformation and lateral migration in microvessels. *Ann Biomed Eng.* 2007; 35:755–765. [PubMed: 17380392]
11. Zhao Y, Chien S, Skalak R, Lipowsky HH. Leukocyte rolling in rat mesentery venules: distribution of adhesion bonds and the effects of cytoactive agents. *Ann Biomed Eng.* 2001; 29:360–372. [PubMed: 11400718]
12. Amos PJ, Shang H, Bailey AM, Taylor A, Katz AJ, Peirce SM. The role of human adipose-derived stromal cells in inflammatory microvascular remodeling and evidence of a perivascular phenotype. *Stem Cells.* 2008; 26:2682–2690. [PubMed: 18436860]

13. Anderson CR, Hastings NE, Blackman BR, Price RJ. Capillary sprout endothelial cells exhibit a CD36low phenotype. *Am J Pathol.* 2008; 173:1220–1228. [PubMed: 18772338]
14. Anderson CR, Ponce AM, Price RJ. Absence of OX-43 antigen expression in invasive capillary sprouts: identification of a capillary sprout-specific endothelial phenotype. *Am J Physiol Heart Circ Physiol.* 2003; 286:H346–H353. [PubMed: 14512284]
15. Murfee W, Skalak T, Peirce S. Differential arterial/venous expression of NG2 proteoglycan in perivascular cells along microvessels: identifying a venule-specific phenotype. *Microcirculation.* 2005; 12 : 151–160. [PubMed: 15824037]
16. Nehls V, Denzer K, Drenckhahn D. Pericyte involvement in capillary sprouting during angiogenesis in situ. *Cell Tissue Res.* 1992; 270:469–474. [PubMed: 1283113]
17. Norrby K Basic fibroblast growth factor and de novo mammalian angiogenesis. *Microvasc Res.* 1994; 48:96–113. [PubMed: 7527478]
18. Woolard J, Wang WY, Bevan HS, et al. VEGF165b, an inhibitory vascular endothelial growth factor splice variant: mechanism of action, in vivo effect on angiogenesis and endogenous protein expression. *Cancer Res.* 2004; 64:7822–7835. [PubMed: 15520188]
19. Zeller PJ, Skalak TC, Ponce AM, Price RJ. In vivo chemotactic properties and spatial expression of PDGF in developing mesenteric microvascular networks. *Am J Physiol Heart Circ Physiol.* 2001; 280 : H2116–H2125. [PubMed: 11299213]
20. Murfee WL. Implications of fluid shear stress in capillary sprouting during adult microvascular network remodeling. *Mechanobiol Endothel.* 2015; 166:184.
21. Murfee WL, Van Gieson EJ, Price RJ, Skalak TC. Cell proliferation in mesenteric microvascular network remodeling in response to elevated hemodynamic stress. *Ann Biomed Eng.* 2004; 32:1662–1666. [PubMed: 15675679]
22. Van Gieson EJ. Enhanced smooth muscle cell coverage of microvessels exposed to increased hemodynamic stresses in vivo. *Circ Res.* 2003; 92:929–936. [PubMed: 12663481]
23. Stapor PC, Murfee WL. Spatiotemporal distribution of neurovascular alignment in remodeling adult rat mesentery microvascular networks. *J Vasc Res.* 2012; 49:299–308. [PubMed: 22538935]
24. Norrby K In vivo models of angiogenesis. *J Cell Mol Med.* 2006; 10:588–612. [PubMed: 16989723]
25. Hague S, Manek S, Oehler MK, MacKenzie IZ, Bicknell R, Rees MC. Tamoxifen induction of angiogenic factor expression in endometrium. *Br J Cancer.* 2002; 86:761. [PubMed: 11875740]
26. Helgestam M, Andersson H, Stavreus-Evers A, Brittebo E, Olovsson M. Tamoxifen modulates cell migration and expression of angiogenesis-related genes in human endometrial endothelial cells. *Am J Pathol.* 2012; 180:2527–2535. [PubMed: 22531128]
27. Rasband WS. ImageJ, U. S. National Institutes of Health, Bethesda, Maryland, USA, <http://rsb.info.nih.gov/ij/>, 1997–2005.
28. Yang M, Aragon M, Murfee WL. Angiogenesis in mesenteric microvascular networks from spontaneously hypertensive versus normotensive rats: angiogenesis in hypertensive rat mesentery. *Microcirculation.* 2011; 18:574–582. [PubMed: 21627712]
29. Motherwell JM, Anderson CR, Murfee WL. Endothelial cell phenotypes are maintained during angiogenesis in cultured microvascular networks. *Sci Rep.* 2018; 8:1–11 [PubMed: 29311619]
30. Ribatti D, Crivellato E. “Sprouting angiogenesis”, a reappraisal. *Dev Biol.* 2012; 372:157–165. [PubMed: 23031691]
31. Gerhardt H, Golding M, Fruttiger M, et al. VEGF guides angiogenic sprouting utilizing endothelial tip cell filopodia. *J Cell Biol.* 2003; 161:1163–1177. [PubMed: 12810700]
32. Geudens I, Gerhardt H. Coordinating cell behaviour during blood vessel formation. *Development.* 2011; 138:4569–4583. [PubMed: 21965610]
33. Chappell JC, Wiley DM, Bautch VL. Regulation of blood vessel sprouting. *Semin Cell Dev Biol.* 2011; 22:1005–1011. [PubMed: 22020130]
34. Norrby K, Jakobsson A, Sörbo J. Mast-cell secretion and angiogenesis, a quantitative study in rats and mice. *Virchows Arch. B* 1989; 57:251. [PubMed: 2474890]
35. Anghelina M, Moldovan L, Moldovan NI. Preferential activity of Tie2 promoter in arteriolar endothelium. *J Cell Mol Med.* 2005; 9:113–121. [PubMed: 15784169]

36. Calderone V, Gallego J, Fernandez-Miranda G. Sequential functions of CPEB1 and CPEB4 regulate pathologic expression of vascular endothelial growth factor and angiogenesis in chronic liver disease. *Gastroenterology*. 2016; 150:982–997. [PubMed: 26627607]
37. Van Steenkiste C, Geerts A, Vanheule E. Role of placental growth factor in mesenteric neoangiogenesis in a mouse model of portal hypertension. *Gastroenterology*. 2009; 137:2112–2124. e6. [PubMed: 19751735]
38. Nagy JA, Masse EM, Herzberg KT, et al. Pathogenesis of ascites tumor growth: vascular permeability factor, vascular hyperpermeability, and ascites fluid accumulation. *Cancer Res*. 1995; 55:360–368. [PubMed: 7812969]
39. Jeon B-H, Jang C, Han J, et al. Profound but dysfunctional lymphangiogenesis via vascular endothelial growth factor ligands from CD11b+ macrophages in advanced ovarian cancer. *Cancer Res*. 2008; 68:1100–1109. [PubMed: 18281485]
40. Bardaa S, Moalla D, Ben Khedir S, Rebai T, Sahnoun Z. The evaluation of the healing proprieties of pumpkin and linseed oils on deep second-degree burns in rats. *Pharm Biol*. 2016; 54:581–587. [PubMed: 26186459]
41. Valacchi G, Lim Y, Belmonte G, et al. Ozonated sesame oil enhances cutaneous wound healing in SKH1 mice: ozonated sesame oil enhances wound healing. *Wound Repair Regen*. 2011; 19:107–115. [PubMed: 21134039]
42. Suarez-Martinez AD, Bierschenk S, Huang K, et al. A novel ex vivo mouse mesometrium culture model for investigating angiogenesis in microvascular networks. *J Vasc Res*. 2018; 55:125–135. [PubMed: 29779031]
43. Carmeliet P. Angiogenesis in life, disease and medicine. *Nature*. 2005; 438:932–936. [PubMed: 16355210]
44. Azimi MS, Myers L, Lacey M, et al. An ex vivo model for anti-angiogenic drug testing on intact microvascular networks. *PLoS ONE*. 2015; 10:e0119227. [PubMed: 25742654]
45. Sweat RS, Sloas DC, Murfee WL. VEGF-C induces lymphangiogenesis and angiogenesis in the rat mesentery culture model. *Microcirculation*. 2014; 21:532–540. [PubMed: 24654984]
46. Motherwell JM, Azimi MS, Spicer K, et al. Evaluation of arteriolar smooth muscle cell function in an ex vivo microvascular network model. *Sci Rep*. 2017; 7:2195. [PubMed: 28526859]
47. Murfee WL, Rehorn MR, Peirce SM, Skalak TC. Perivascular cells along venules upregulate NG2 expression during microvascular remodeling. *Microcirculation*. 2006; 13:261–273. [PubMed: 16627368]
48. Sweat RS, Sloas DC, Stewart SA, et al. Aging is associated with impaired angiogenesis, but normal microvascular network structure, in the rat mesentery. *Am J Physiol Heart Circ Physiol*. 2017; 312:1275–1284.

**FIGURE 1.**

Growth of microvascular networks in mouse mesentery. PECAM labeling identified endothelial cells along microvascular networks. Mouse mesentery tissue from 21 d post-injection with saline (A), non-sterile sunflower oil (B), and tamoxifen (C); scale bars = 200 μ m. The solid lines denote the border between the connective tissue and the adipose tissue (+). Bright field image shows perfused microvasculature (D) from sterile sunflower oil within the mesenteric window (dashed lines); scale bar = 1 mm. The quantification of vascularized tissue area (E) and vascular density (F) from each group is shown. A = arteriole, V = venule, and C = capillary. Data are shown as the mean + SEM, n = 8. The * and *** represent $P < 0.05$ and $P < 0.0001$, respectively

**FIGURE 2.**

Multiple cell types are present in the vascularized mouse mesentery tissues 21 d post sunflower oil stimulation. Mouse mesentery tissues have PECAM-positive endothelial cells comprising microvascular networks (A-O), along with supporting cells including α SMA-positive smooth muscle cells (A-C), NG 2-positive pericytes (D-F), and CD 11b-positive macrophages (M-O). In addition to blood vessels, LYVE-1-positive (G-I) and Prox1-positive (J-L) lymphatic vessels are also present. A = arteriole, V = venule, and L = lymphatic. Arrows identify wrapping pericytes. Arrowheads identify interstitial macrophages. Scale bars = 100 μ m

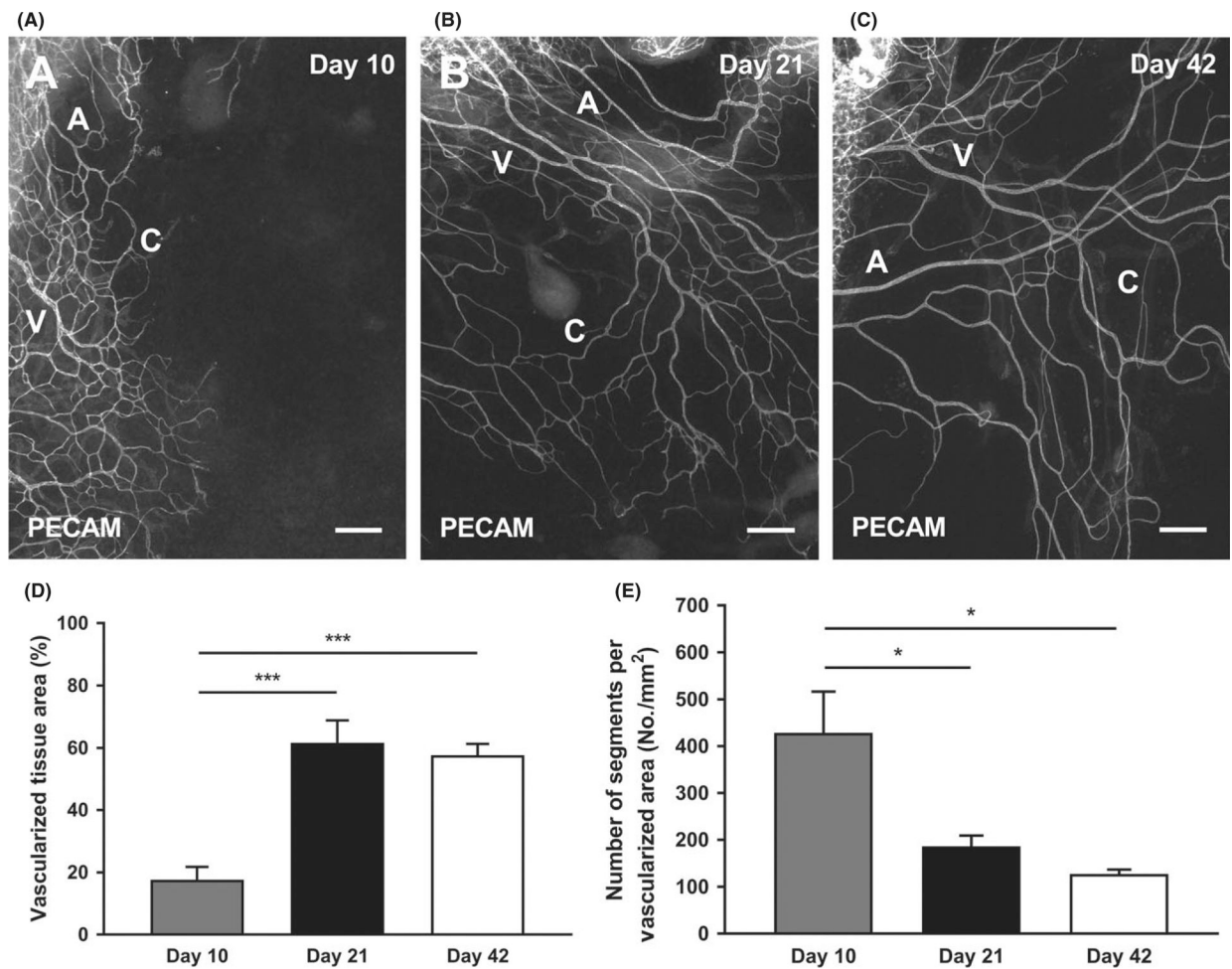


FIGURE 3.

Growth of microvascular networks in mouse mesentery after 10, 21, and 42 d post sterile sunflower oil stimulation. PECAM labeling identified endothelial cells along microvascular networks Day 10 (A), Day 21 (B), and Day 42 (C) post-injection with sunflower oil. The quantification of vascularized tissue area (D) and vascular density (E) from the different days is shown. A = arteriole, V = venule, and C = capillary. Data are shown as the mean + SEM, n = 8. The * and *** represent $P < 0.05$ and $P < 0.0001$, respectively. Scale bars = 200 μm

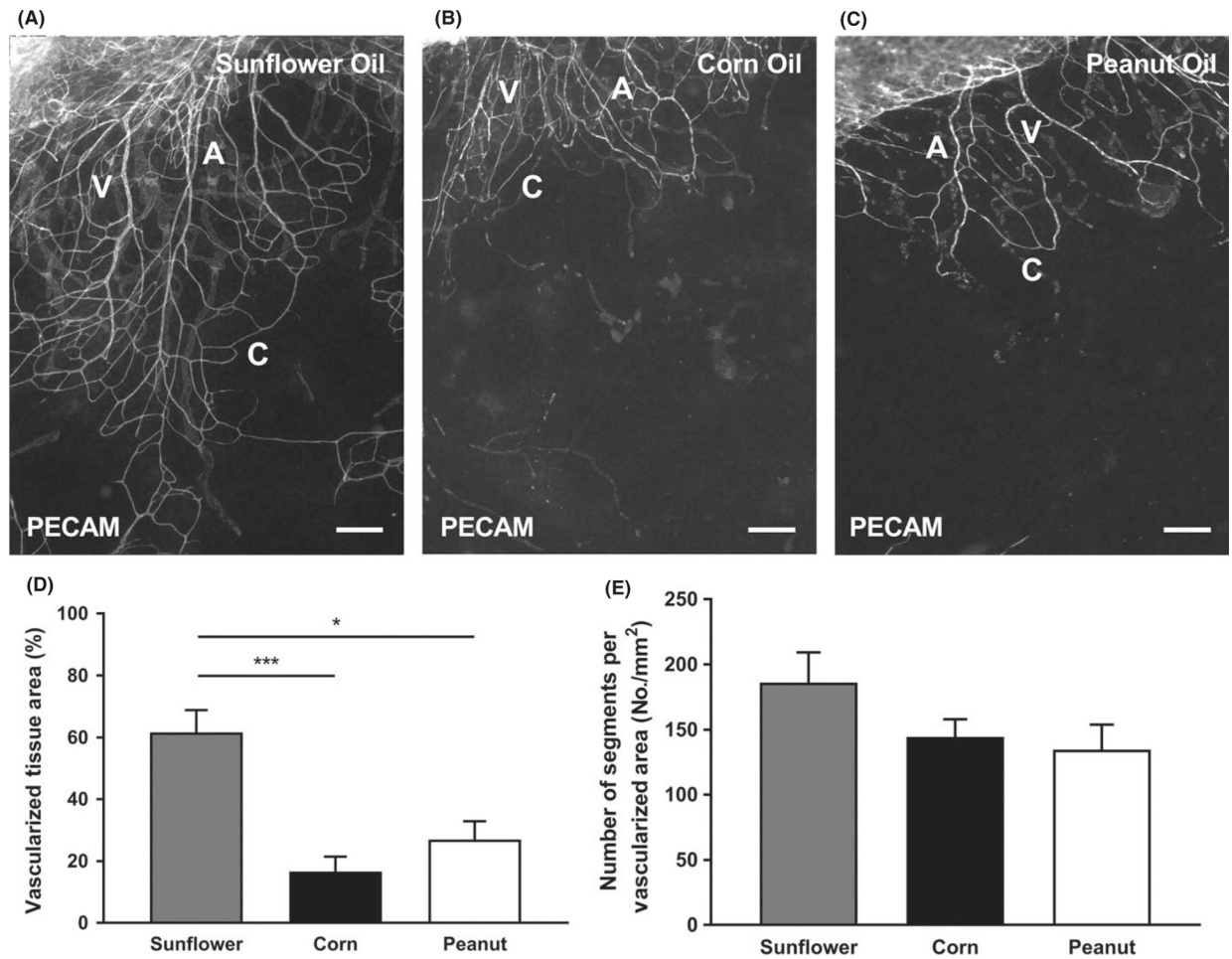


FIGURE 4.

Various sterile oil stimulations induce growth of microvasculature in the mouse mesentery. PECAM labeling identified endothelial cells along microvascular networks. Mouse mesentery tissue from 21 d post-injection with Sunflower Oil (A), Corn Oil (B), and Peanut Oil (C). The quantification of vascularized tissue area (D) and vascular density (E) from the different oils is shown. A = arteriole, V = venule, and C = capillary. Data are shown as the mean + SEM, n = 8. The * and *** represent $P < 0.05$ and $P < 0.0001$, respectively. Scale bars = 200 μm

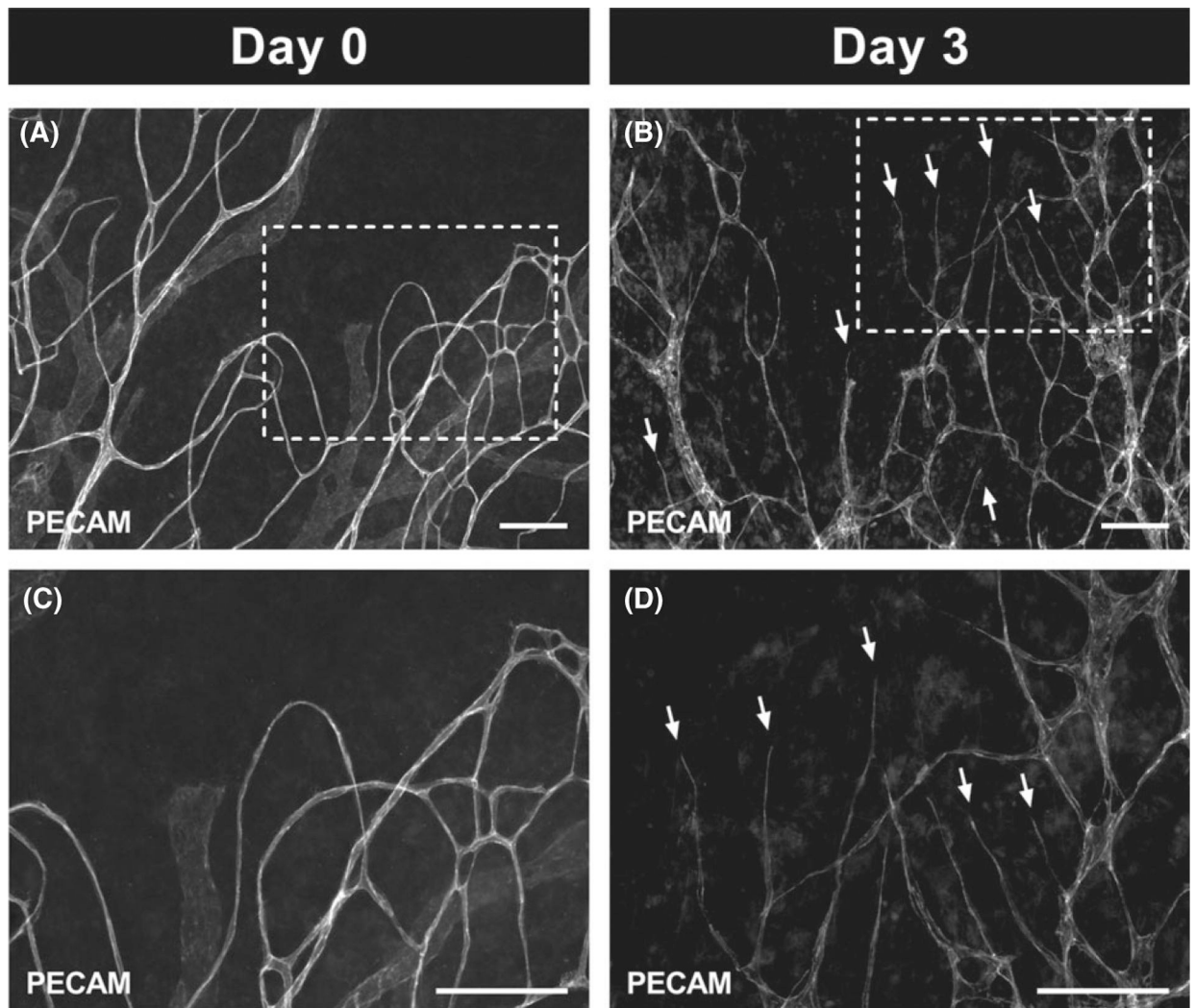
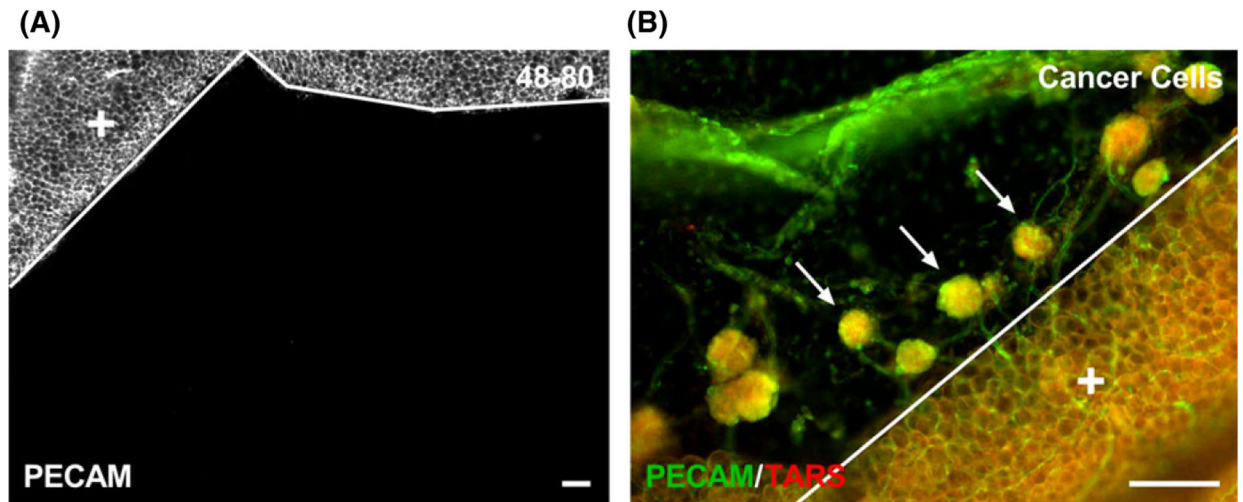


FIGURE 5.

Angiogenesis can be stimulated during culture in microvascular networks from mouse mesentery tissues after 21 d post sterile sunflower oil stimulation. Tissues cultured with MEM supplemented with 20% FBS for 3 d (B, D) had an obvious angiogenic response indicated by the capillary sprouts (arrows) when compared to tissues which had not been cultured (A, C). Images C and D are higher magnification of the images in A and B demarcated by the dashed rectangles. Scale bars = 100 μ m

**FIGURE 6.**

Different stimuli have different effects on microvascular growth in the mouse mesentery. After giving an IP injection of 0.5 mL doses of compound 48–80 (40, 80, 120, 160, and 200 $\mu\text{g}/\text{mL}$ in sterile saline) over the time course of 3 d (twice a day and once on the last day) in increasing concentrations to adult, female C57 BL /6 mice ($n = 2$), PECAM-positive microvessels were not identified after 10 d post-injection (A). PECAM-positive endothelial cells comprising microvessels were observed after 4 wk of injected transformed mouse ovarian epithelial cells (3×10^6 cells in 0.2 mL of PBS), where spheroid tumors contained microvasculature into the mesenteric window (B). Arrows identify spheroid tumors which are comprised of TARS-positive cells. The solid lines denote the border between the connective tissue and the adipose tissue (+). Scale bars = 100 μm